EJC Paediatric Oncology 2 (2023) 100122

Contents lists available at ScienceDirect

EJC Paediatric Oncology

journal homepage: www.journals.elsevier.com/ejc-paediatric-oncology

Diagnostic MRI characteristics of pediatric clear cell sarcoma of the kidney and rhabdoid tumor of the kidney: A retrospective multi-center SIOP-RTSG Radiology panel study

Justine N. van der Beek [a,b,*], Jens-Peter Schenk [c], Tom A. Watson [d], Ana Coma [e], Carlo Morosi [f], Norbert Graf [g], Tanzina Chowdhury [h], Gema L. Ramírez-Villar [i], Filippo Spreafico [j], Kristina Dzhuma [k,l], Lidwine B. Mokkink [m,n], Ronald R. de Krijger [b,o], Marry M. van den Heuvel-Eibrink [b,p], Annemieke S. Littooij [a,b]

[a] Department of Radiology and Nuclear Medicine, University Medical Center Utrecht/Wilhelmina Children's Hospital, Utrecht University, Utrecht, the Netherlands
[b] Princess Máxima Center for Pediatric Oncology, Utrecht, the Netherlands
[c] Clinic of Diagnostic and Interventional Radiology, Division of Pediatric Radiology, Heidelberg University Hospital, Heidelberg, Germany
[d] Department of Paediatric Radiology, Great Ormond Street Hospital for Children NHS Foundation Trust, London, United Kingdom
[e] Department of Pediatric Radiology, Hospital Vall d'Hebron, Barcelona, Spain
[f] Department of Radiology, Fondazione IRCCS Istituto Nazionale dei Tumori, Milan, Italy
[g] Department of Pediatric Oncology & Hematology, Saarland University Medical Center and Saarland University Faculty of Medicine, Homburg, Germany
[h] Department of Haematology and Oncology, Great Ormond Street Hospital for Children NHS Foundation Trust, London, United Kingdom
[i] Department of Paediatric Oncology, Hospital Universitario Virgen del Rocío, Seville, Spain
[j] Pediatric Oncology Unit, Department of Medical Oncology and Hematology, Fondazione IRCCS Istituto Nazionale dei Tumori, Milan, Italy
[k] Developmental Biology and Cancer Department, University College London Great Ormond Street Institute of Child Health, London, United Kingdom
[l] Department of Paediatric Urology, Great Ormond Street Hospital for Children NHS Foundation Trust, London, United Kingdom
[m] Department of Epidemiology and Data Science, Amsterdam UMC, Vrije Universiteit Amsterdam, Amsterdam, the Netherlands
[n] Amsterdam Public Health Research Institute, Amsterdam, the Netherlands
[o] Department of Pathology, University Medical Center Utrecht, Utrecht, the Netherlands
[p] Division of Child Health, Wilhelmina Children's Hospital, Utrecht University, Utrecht, the Netherlands

ARTICLE INFO

Keywords:
Kidney neoplasms
Clear cell sarcoma
Rhabdoid tumor
Wilms tumor
Radiology
Magnetic resonance imaging
Pediatrics

ABSTRACT

Introduction: Clear cell sarcoma of the kidney (CCSK) and rhabdoid tumor of the kidney (RTK) are rare malignant pediatric renal tumors, both accounting for 1–5% of diagnoses. Within the International Society of Pediatric Oncology-Renal Tumor Study Group (SIOP-RTSG) protocols diagnostic invasive procedures to determine histology are discouraged. MRI has become the preferred imaging modality, however, non-invasive discrimination of CCSK and RTK remains challenging. Therefore, this study aims to identify diagnostic MRI-characteristics of CCSK and RTK, in the largest series of patients to date.

Material and methods: Five SIOP-RTSG national review radiologists identified national diagnostic MRIs of histologically proven CCSKs and RTKs. Scan-protocols were based on MRI-guidelines following SIOP-RTSG protocols. Radiologists assessed their national cases using a validated case report form (CRF).

Results: Retrospectively, 59 patients were identified ($n = 38$ CCSK, $n = 21$ RTK). CCSKs showed a high median volume (576 cm^3, range 54–4414), which was lower for RTKs (290 cm^3, range 20–761) ($p = 0.006 * 10^{-3}$). Fifty-two percent (11/21) of RTK-patients showed disease at other locations, predominantly the lungs and brain, compared to 8% of CCSK-patients (3/38). RTKs showed ill-defined margins (12/21, 57%) and infiltrative growth pattern (13/21, 62%). CCSKs appeared hyper-intense on T2-weighted imaging (27/38, 71%) with a characteristics band-like enhancement (13/38, 34%), whereas RTK cases often showed T2-weighted hypo-intensity (11/21, 52%). The overall mean ADC-value for CCSK was $1.11 * 10^{-3}$ mm^2/s (range 0.57–2.07 $*10^{-3}$ mm^2/s), and $0.72 * 10^{-3}$ mm^2/s (range 0.53–0.90 $*10^{-3}$ mm^2/s) for RTK.

Conclusions: This retrospective study suggests a small size, T2-weighted hypo-intensity and an aggressive growth pattern may be characteristic for RTK. CCSK often showed a typical band-like enhancement pattern with

* Correspondence to: UMC Utrecht, Heidelberglaan 100, 3584 CX Utrecht, the Netherlands.
E-mail address: j.n.vanderbeek-6@umcutrecht.nl (J.N. van der Beek).

https://doi.org/10.1016/j.ejcped.2023.100122
Received 30 June 2023; Received in revised form 24 October 2023; Accepted 26 October 2023
Available online 4 November 2023

relatively high ADC-values. Identified MRI-characteristics may be used in future studies focusing on validation and discrimination from especially WT, aiming for an early non-invasive diagnosis.

1. Introduction

Pediatric renal tumors account for approximately 6% of childhood malignancies [1,2]. The majority of these patients is diagnosed with a Wilms tumor (WT), with a peak incidence around three years of age [3,4]. Nevertheless, there are also other, more rare, non-WTs, presenting at a young age [3–6]. Rhabdoid tumors of the kidney (RTK) present predominantly in the first three years of life, accounting for roughly 1–4% of renal tumor diagnoses in children [7–11]. Similarly, clear cell sarcomas of the kidney (CCSK), comprising approximately 1–5% of pediatric renal tumor diagnoses, show the highest incidence in children up to 4 years [5,12–14].

Pre-operative chemotherapy without tumor biopsy is standard of care for children with renal tumors between 6 months and 10 years of age according to the current Renal Tumor Study Group of the International Society of Pediatric Oncology (SIOP-RTSG) 2016 UMBRELLA protocol, given the vast predominance of WTs in this age range. Preferably, non-WTs could be identified at diagnosis as they may benefit from different treatment approaches [1,15]. Nevertheless, invasive procedures to determine histology before the start of therapy in young children are discouraged. According to previous literature and experience which have informed the current SIOP-RTSG guidelines, renal tumor patients are selected for pre-treatment core-needle biopsy if they fulfill criteria relating to an unusual clinical presentation and/or imaging findings suspicious for a non-WT, such as calcifications, lymphadenopathy, renal parenchyma that is not visible or an almost totally extra-renal processes [15–17].

However, non-invasive discrimination of pediatric renal tumor subtypes remains challenging, as numbers are low and blind prediction studies are not available to date. Nevertheless, Ueno-Yokohata et al. showed detection of BCOR internal tandem duplication through liquid biopsy might enable less invasive pre-operative diagnosis of CCSK [18]. Furthermore, available imaging studies showed that RTK and CCSK share multiple common features with WTs [19–21]. All three can present as rather large, heterogeneous enhancing masses with lung metastases [6,12,22,23]. Previous studies however indicated that subcapsular fluid, calcifications and synchronous central nervous system (CNS) tumors could be suggestive for RTK [10,24]. Also, CCSK historically tends to metastasize to the bone [14,25,26]. Despite these associated clinical characteristics studies focusing on imaging of these rare pediatric renal tumors have not identified radiological features which robustly distinguish different entities. Also, studies have mainly included cross-sectional computed tomography (CT), whereas magnetic resonance imaging (MRI) has become the preferred imaging modality within the SIOP-RTSG [1,27]. MRI has a potential value as non-invasive biomarker, with a lack of ionizing radiation and excellent soft-tissue contrast [28,29].

Studies focusing on MRI-characteristics of RTK and CCSK remain limited. Nonetheless, identification of specific MRI-characteristics of these non-WTs at diagnosis is important for future studies focusing on the comparison with WTs [30]. CCSK and RTK are highly aggressive and usually need a more intensive treatment approach compared to WT, indicating that upfront discrimination of these rare tumors from each other, but even more importantly from WT, might have important implications for initial treatment. Therefore, non-invasive identification at presentation may be beneficial for better outcome [10,22,26,31,32]. This study aims to identify MRI-characteristics of prospectively registered CCSK- and RTK cases at diagnosis through a retrospective international multicenter cohort study, thereby describing imaging findings of the largest number of patients to date.

2. Material and methods

2.1. Patients

For this study, five SIOP-RTSG national review radiologists searched their databases for pediatric patients (0–18 years), diagnosed with histologically proven CCSK or RTK after biopsy or surgery. All patients were registered in SIOP (2001 or 2016 UMBRELLA) or UK-IMPORT (Improving Population Outcomes for Renal Tumours of childhood) databases. Available cases were included when a diagnostic MRI-scan was available and performed as standard of care following SIOP-RTSG protocols. Histopathological assessment of the included cases was assessed by national SIOP-RTSG pathologists following the currently active SIOP-RTSG protocols [33–36].

2.2. Magnetic resonance imaging acquisition

Children were scanned in their treating national center within Germany, The Netherlands, the United Kingdom, Spain and Italy. Scan protocols were based on the MRI-guidelines within SIOP-RTSG protocols on 1.5-T systems (Supplementary Table 1). The sequences and scan parameters recommend by the SIOP-RTSG in the current 2016 UMBRELLA protocol for MRI of pediatric renal tumors were recently reported by Watson et al. and van der Beek and Artunduaga et al. [16,27]. When diffusion weighted imaging (DWI) was available, the apparent diffusion coefficient (ADC) maps were in the majority calculated based on b-values of 0/800, 0/100/1000 or 50/400/800 (Supplementary Table 1).

Children were awake, sedated or under general anesthesia depending on their ability to cooperate, according to local standard of care procedures. Administration of gadolinium and Hyoscine butylbromide was performed according to center specific regulations, based on the current general recommendations of the SIOP-RTSG/UK-IMPORT protocols [27].

2.3. Image analysis and case report form

The five radiologists (JPS with 20 years of experience, ASL with 15 years of experience, TAW with 11 years of experience, AC with 10 years of experience and CM with 20 years of experience) assessed their national CCSK- and RTK cases through a case report form (CRF). This captured MRI-characteristics of diagnostic MRI-scans of pediatric renal tumors supported by an instruction file (Supplementary File 1, Supplementary File 2). CRFs were anonymized through specific IDs for each country by the national radiologists, and shared without the anonymization key with the lead investigator. Tumor volumes were statistically analyzed with the Mann-Whitney U-test in SPSS, version 27.0.

The content of the CRF was predominantly based on the results of a recent SIOP-RTSG Radiology panel Delphi study [20]. To allow international use, an interrater agreement study was performed prior to the start of this retrospective study, in which 15 randomly selected pediatric WT-patients with a representative range of patient characteristics were assessed by the 5 involved radiologists. Agreement for each MRI-characteristic in the CRF was analyzed through percentages of observed and specific agreement for dichotomous and ordinal characteristics and standard error of measurement for agreement through a two-way random effects model for continuous characteristics. Reliability was analyzed through (weighted) Cohen's kappa (κ) for dichotomous and ordinal characteristics and intra-class correlation coefficients (ICC) for continuous characteristics [37–41]. The aim of this analysis was to identify MRI-characteristics in the CRF that might need

improvement or rewriting, and to show acceptable agreement of characteristics based on collaborative expert judgment (Supplementary Table 2) [42]. Furthermore, based on literature, ICCs > 0.75 were considered excellent, whereas κ-values > 0.6 were interpreted as substantial, although high reliability was not expected given the small sample size and homogeneous patient population [43].

Characteristics, including their descriptions, that reached unsatisfactory results, were collectively discussed and rewritten in two consecutive rounds resulting in a CRF with satisfactory agreement for all MRI-characteristics among five raters (Supplementary Table 2). In this way, all individual radiologists were able to assess their own national CCSK- and RTK cases, without need for data-sharing agreements and without need for two observers per patient.

3. Results

3.1. Patient characteristics

Fifty-nine patients from five countries were included (Germany (n = 16), The Netherlands (n = 13) United Kingdom (n = 14), Spain (n = 8) and Italy (n = 8)) (Supplementary Table 1, Table 1).

Thirty-eight patients had CCSK, whereas 21 patients were diagnosed with RTK. The median age for CCSK was 2.7 years (range 5–122 months), and the median age for RTK was 0.4 years (range 1–38 months). Thirty-two/38 (84%) and 11/21 (52%) of the CCSK- and RTK-patients, respectively, were male (Table 1). Eleven RTK-patients (52%) had metastatic and/or synchronous disease at diagnosis, with the lungs (6/11, 55%) and brain (4/11, 36%) as most common sites, whereas 3/38 (8%) CCSK-patients showed metastases in para-aortic lymph nodes, bones and/or liver and lungs on imaging at diagnosis (Table 1, Fig. 1).

3.2. General tumor characteristics and growth pattern

The majority of CCSKs (23/38, 61%) as well as RTKs (19/21, 90%) were located centrally in the kidney (Table 1). The median tumor volume of CCSKs was 576 cm^3 (range 54–4414 cm^3), whereas RTKs were significantly smaller ($p = 0.006 * 10^{-3}$), with a median tumor volume at diagnosis of 290 cm^3 (range 20–761 cm^3). In RTK enlarged regional lymph nodes were observed in 11/21 (52%) of the cases, and in CCSK patients this was observed in 3/38 (8%) cases (Table 1).

Concerning growth pattern, tumor margins of RTK were ill-defined in the majority of the identified cases (12/21, 57%), in line with a majority of the cases showing an infiltrative growth pattern (13/21, 62%) (Fig. 1). Only 3/21 (14%) RTKs showed a pseudo-capsule, and just one patient had an indication of intra-peritoneal spread on MRI (Table 1). Almost all CCSKs (31/32, 82%) showed a pseudo-capsule, with 35/38 (92%) cases with well-defined tumor margins, but also 14/38 (37%) tumors indicating a breach of their capsule (Fig. 2). In total, only 5/59 patients (8%) showed venous invasion (Table 1).

3.3. Solid tumor characteristics

On T2-weighted (T2W) imaging, both CCSK and RTK predominantly showed T2W heterogeneity (63% and 90%, respectively). The majority of CCSKs (27/38, 71%) was hyper-intense on T2W imaging compared to healthy renal cortex (Fig. 2). RTKs were mainly T2W hypo-intense (11/21, 52%) (Fig. 1). Concerning T1-weighted (T1W) imaging, both tumors showed hypo-intensity and heterogeneity in most of the cases. On contrast-enhanced T1W imaging, in both tumors 19 patients showed a heterogeneous pattern (50% of CCSKs, 90% of RTKs), whereas 13/38 (34%) of CCSKs showed typical band-like areas of late or non-enhancement (Table 1, Fig. 2).

In line with the heterogeneous pattern of both tumor types, hemorrhage and necrosis was seen in 20/38 (53%) of CCSK cases and 14/21 (67%) of RTK cases. Cysts in these tumors were limited, as well as minor cases with subcapsular fluid for both CCSKs (7/38, 18%) and RTKs (4/21, 19%). None of the tumors showed fatty tissue on MRI (Table 1).

Table 1
Magnetic resonance imaging (MRI)-characteristics of the included pediatric patients with clear cell sarcoma of the kidney (CCSK) and rhabdoid tumor of the kidney (RTK).

Characteristics		CCSK (n = 38)	RTK (n = 21)
Origin of included patients	Germany	11	5
	The Netherlands	6	7
	United Kingdom	11	3
	Spain	5	3
	Italy	5	3
Clinical characteristics	Median age *(months)*	32 (5–122)	5 (1–38)
	Sex *(male)*	32 (84%)	11 (52%)
	Tumor side *(right)*	23 (61%)	9 (43%)
	Metastatic disease	3 (8%)	11 (52%)
	Site of metastases (number of patients)	*Lu*(1), *Li*(1), *Bo*(1), *LN*(1)	*Lu*(6), *Br*(4), *Li*(1), *M*(1)
General tumor characteristics on MRI	Median tumor volume *(cm^3, range)*	576 (54–4414)	290 (20–761)
	Location of the tumor		
	·Central	23 (61%)	19 (90%)
	·Peripheral	8 (21%)	2 (10%)
	·Indistinguishable	7 (18%)	0 (0%)
	Regional lymph nodes	6 (16%)	11 (52%)
Growth pattern on MRI	Tumor margins *(well-defined / ill-defined)*	35 (92%) / 3 (8%)	9 (43%) / 12 (57%)
	(Pseudo)capsule	31 (82%)	3 (14%)
	Breach of the tumor capsule	14 (37%)	6 (29%)
	Intra-peritoneal spread	0 (0%)	1 (5%)
	Infiltrative growth pattern	5 (13%)	13 (62%)
	Venous invasion / Tumor thrombus	3 (8%)	2 (10%)
	T2-weighted pattern		
Solid tumor characteristics on MRI	·Homogeneous	14 (37%)	2 (10%)
	·Heterogeneous	24 (63%)	19 (90%)
	T2-weighted intensity	27 (71%)	2 (10%)
	·Hyper-intense	1 (3%)	11 (52%)
	·Hypo-intense	10 (26%)	6 (28%)
	·Iso-intense	0 (0%)	2 (10%)
	·Hypo- and iso-intense		
	T1-weighted pattern		
	·Homogeneous	14 (37%)	3 (14%)
	·Heterogeneous	24 (63%)	18 (86%)
	T1-weighted intensity	0 (0%)	1 (5%)
	·Hyper-intense	36 (95%)	13 (62%)
	·Hypo-intense	2 (5%)	6 (28%)
	·Iso-intense	0 (0%)	1 (5%)
	·Hypo- and iso-intense		
	Hemorrhage / Necrosis	20 (53%)	14 (67%)
	·Limited	13 (65%)	9 (64%)
	·More extensive	7 (35%)	5 (36%)
	Cysts	12 (32%)	8 (38%)
	Fatty tissue	0 (0%)	0 (0%)
	Subcapsular fluid	7 (18%)	4 (19%)
	Increased vascularity	9 (24%)	1 (5%)
	Enhancement pattern		
	·Homogeneous	3 (8%)	0 (0%)
	·Heterogeneous	19[a] (50%)	19[b] (90%)
	·Band-like areas	13 (34%)	2 (10%)
	(heterogeneous)	3 (8%)	0 (0%)
	·No enhancement		
Diffusion weighted imaging	Median overall ADC-value *($*10^{-3}$ mm^2/s, range)*	1.11 (0.57–2.07)	0.72 (0.53–0.90)

MRI = magnetic resonance imaging; Lu = Lungs; Li = Liver; Bo = Bones; LN = Lymph nodes; Br = Brain; M = Mediastinum.
[a] Two patients showed central necrosis with peripheral homogeneous enhancement;
[b] Three patients showed nodular heterogeneous enhancement

3.4. Diffusion weighted imaging

In 50/59 (85%) cases DWI was available to evaluate mean ADC-

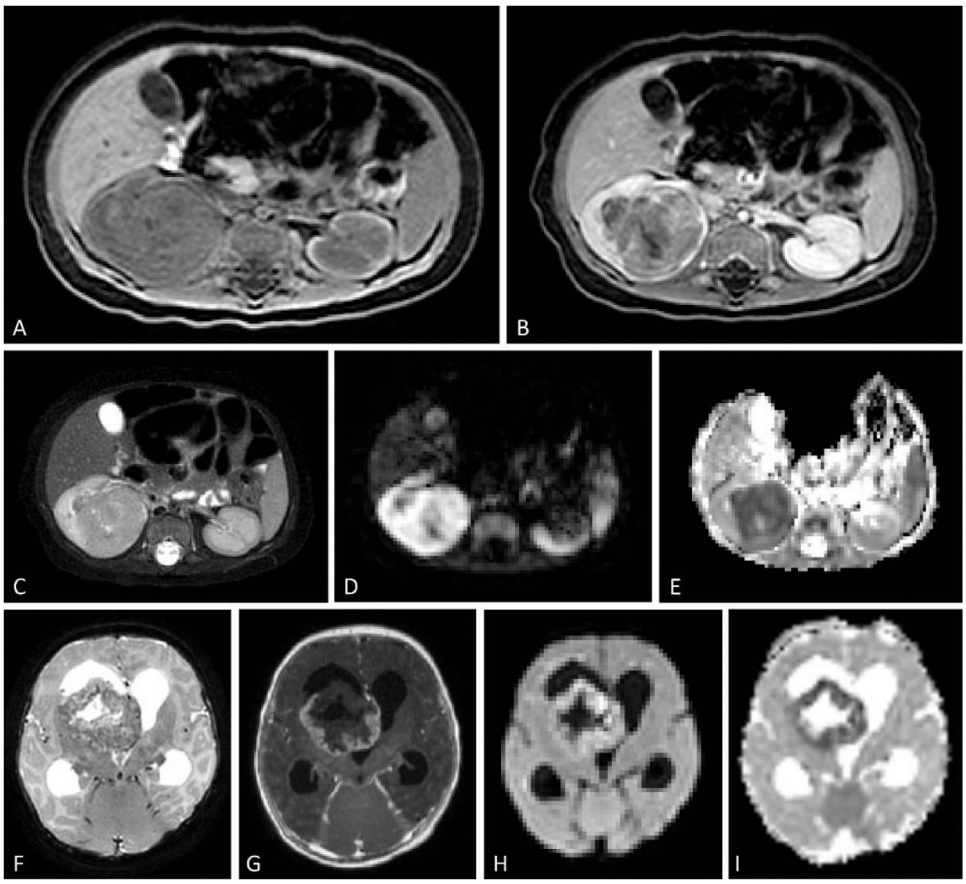

Fig. 1. Diagnostic magnetic resonance imaging (MRI) of a 3-month-old female patient with a right-sided rhabdoid tumor of the kidney (RTK) and synchronous brain tumor. A 3-month-old female patient presented with a small right-sided renal tumor (29 cc) with ill-defined margins. On T1-weighted (T1W) imaging without (A) and with (B) contrast, the tumor showed hypo-intensity and a heterogeneous enhancement. On T2-weighted (T2W) imaging with fat suppression (C), the tumor appeared homogeneous and hypo- to iso-intense, with a few scattered cysts. The tumor showed a low mean apparent diffusion coefficient (ADC) of 0.71 * 10^{-3} mm^2/s (range of drawn ROIs 0.67–0.76 *10^{-3} mm^2/s), illustrated on the diffusion weighted imaging (DWI) b400- (D) and ADC-map (E). An MRI of the brain showed a synchronous brain tumor (4.6 ×3.9 ×4.7 cm) with T2W hypo-intensity and heterogeneity (F), and a strong enhancement of especially the borders of the tumor on T1W contrast-enhanced imaging (G). On DWI, the b1000- (H) and ADC-map (I) confirmed high cellularity of the tumor borders, showing strong diffusion restriction.

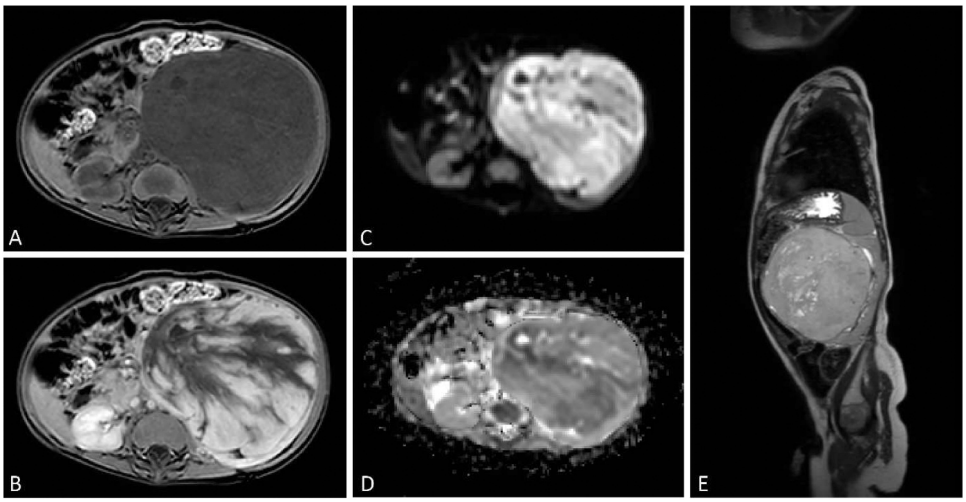

Fig. 2. Diagnostic magnetic resonance imaging (MRI) of a 7-month-old male patient with a left-sided clear cell sarcoma of the kidney (CCSK). A 7-month-old male patient presented with a large left-sided renal tumor (419 cc) with well-defined margins and a tumor capsule. On T1-weighted (T1W) imaging (A) the tumor appeared homogeneous and hypo-intense, with a characteristic band-like enhancement pattern on T1W contrast-enhanced imaging (B). Diffusion weighted imaging (DWI) showed limited diffusion restriction based on the b1000- (C) and apparent diffusion coefficient (ADC)-map (D), with a mean ADC of 1.12 * 10^{-3} mm^2/s (range of drawn ROIs 1.10–1.13 *10^{-3} mm^2/s). On the sagittal T2-weighted (T2W) scan (E), the tumor appeared heterogeneous and hyper-intense, with a few peripheral cysts.

values based on ROIs. The overall mean ADC-value for CCSK (30/38, 79%) was 1.11 * 10^{-3} mm^2/s (range 0.57–2.07 *10^{-3} mm^2/s). The overall mean ADC-value for RTK (20/21, 95%) was 0.72 * 10^{-3} mm^2/s (range 0.53–0.90 mm^2/s) (Table 1, Figs. 1, 2).

4. Discussion

This retrospective multicenter study aimed to identify MRI-characteristics of CCSK and RTK. Given the rarity of these malignant pediatric renal tumors and previous focus on CT, overall knowledge of MRI appearance of especially non-WTs in children is still limited (Table 2) [20]. A literature review focusing on MRI-characteristics of CCSK and RTK resulted in only five case reports (Supplementary Table 3, Supplementary Fig. 1, Table 2) [44–48]. Nevertheless, diagnosis and discrimination of different pediatric renal tumor types based on imaging plays an increasingly important role, especially in the SIOP-RTSG setting where treatment with pre-operative chemotherapy without histological confirmation is standard of care [1,27,49]. This descriptive study is the first to illustrate the appearance of CSSK and RTK by MRI only, allowing further studies to focus on exploring the potential use of MRI as a non-invasive biomarker in the field of pediatric renal tumors, especially in the discrimination of these rare non-WTs from WTs.

Concerning patient characteristics, the age of identified patients was in line with previous reports, indicating a majority of the RTK-patients being younger than 2 years old, and a comparable peak incidence with WT around 3 years of age for CCSK (Table 2) [3,4,12,26,45,47,48]. As indicated, discrimination from WTs is difficult, given multiple common features. CCSK as well as WT present as large heterogeneous masses, however, RTK, as also demonstrated in this study, is reported to be smaller at diagnosis [15,17]. In contrast to WTs, which present bilaterally in approximately 4–13% of children, bilateral cases of RTK and CCSK are extremely rare [11,16,19,31,50]. Whereas the initial name of CCSK was 'bone metastasizing tumor of the kidney', only one patient in our series showed skeletal metastases [51–53]. The percentage and location of metastases at diagnosis for CCSK is in line with previous reports, indicating 6–7% metastatic cases, mainly to lungs, liver, lymph nodes and bones [6,12,26]. Together with pulmonary lesions, brain lesions were the most often reported metastases for RTKs. Concurrent or metastatic CNS lesions have been often described as suggestive or even pathognomonic for RTK, related to SMARCB1 deficiency in rhabdoid tumors [7,10,54,55]. Nevertheless, despite the rather specific potential metastatic sites for CCSK and RTK, pulmonary metastases remain most common to both at diagnosis [10,11,56,57].

Whereas several imaging characteristics of CCSK and RTK overlap, the more aggressive infiltrative growth pattern of RTK seems a rather specific imaging characteristic. RTKs were already known as highly invasive and malignant, and this growth pattern was, apart from our cases, also specifically reported in the rare MRI-reports identified in previous literature (Table 2) [46,47,54]. The vast majority of CCSKs showed a (pseudo)capsule with well-defined tumor margins, similar to WTs. Still, several CCSK cases showed a breach of the tumor capsule. Nevertheless, the definition of a capsule rupture has always been under discussion among radiologists, in this study leading to a distinction between a breach of the capsule and actual intraperitoneal spread (Supplementary File 2, Supplementary Table 2) [16,20,58]. Whereas subcapsular fluid has often been reported as potential specific imaging characteristic of non-WTs, and especially of RTKs, it was reported in less than 20% of our cases. [47,59–61] Finally, a tumor thrombus is often referred to as specific for WT, whereas only a small percentage of the CCSK- and RTK-patients described in this study showed venous invasion [16,20].

Both investigated tumor types appeared heterogeneous on T2W and T1W imaging with and without contrast. This was often in relation to presence of hemorrhage and/or necrosis, as also indicated in identified literature (Table 2) [44–48]. Nonetheless, these features are also highly consistent with WTs, which are also notorious for their heterogeneity [50,62,63]. Histologically, CCSK is known as a stromal tumor, mostly showing bland ovoid cells that are arranged in cords and nests separated by a 'chicken-wire vasculature' [6,12,64]. The apparently typical band-like enhancement of these tumors on MRI may be explained by this histological appearance, however, the stromal origin of the tumor also makes discrimination from stromal WT difficult [64]. Whereas CCSK appeared predominantly T2W hyper-intense, similar to WTs, RTK mainly showed T2W hypo-intensity [62,65]. This T2W hypo-intensity is also often described in renal cell carcinomas, which however mostly occur in the second decade of life in children [27,49,66].

DWI is increasingly used in the diagnostic- and response assessment setting of pediatric renal tumors, given its functional and quantitative value. To date, research has predominantly focused on the relevance of ADC-values in WTs, aiming for discrimination of histological WT-subtypes [28,29,67,68]. In this study, single mean ADC-values of representative ROIs were measured, without providing data for calculating accurate median ADC-values, which are more often used in literature (Supplementary File 2). Nevertheless, the lower overall mean ADC-value for RTK appears to be in the range of blastemal and epithelial WT, whereas assessed ADC-values of CCSK, as expected based on histopathology, were close to previously reported ADC-values of stromal type WT [16,28,29,63,67–69].

Our study has a few limitations, mainly based on its retrospective nature and international setting leading to potential information bias and variability. However, the interrater agreement analysis of the CRF allowed the individual radiologists to assess their own national cases in

Table 2
Magnetic resonance imaging (MRI)-characteristics of previously described clear cell sarcomas of the kidney (CCSK) and rhabdoid tumors of the kidney (RTK) in identified studies following a literature review.

Nr.	Author	Nr. of patients	Age	Sex	Appearance on MRI	Metastases
1	Hirose et al. [44]	1 CCSK	9 years	M	Large (11.0 ×10.0 ×8.0 cm) left renal upper pole mass with heterogeneous enhancement of soft tissue and a necrotic and hemorrhagic appearance on T2W	None
2	Trejo et al. [45]	1 CCSK	28 months	M	Large (10 ×7.5 ×7.5 cm) left renal mass with small areas of increased hyperintensity on T2W consistent with necrosis	None
4	Sharma et al. [46]	1 RTK	8 years	M	Large (11.3 ×7.6 ×14.2 cm) right renal mass with diffuse heterogeneity and a tumor thrombus extending into the right renal vein and inferior vena cava	None
5	Eftekhari et al. [47]	1 RTK	18 months	F	Large (11.7 ×8.3 cm) right renal mass with heterogeneous signal intensity on T1W and T2W. Intermediate signal intensity on T1W with interspersed foci of low intensity. Low intensity subcapsular fluid collection with interspersed high intensity suggesting hemorrhage or proteinaceous material. Slight hyperintensity on T2W, with interspersed foci of high intensity suggesting necrosis and low intensity foci suggesting fibrosis.	Pulmonary and nodal metastases
6	Chung et al. [48]	1 RTK	Congenital	NS	Large right renal upper pole mass with heterogeneous T1W and T2W signals consistent with large areas of acute hemorrhage and necrosis.	Medulloblastoma of the posterior fossa

MRI = magnetic resonance imaging; CCSK = clear cell sarcoma of the kidney; RTK = rhabdoid tumor of the kidney; M = male; F = female; T2W = T2-weighted imaging; T1W = T1-weighted imaging; NS = not specified.

the best possible way, given satisfactory and generalizable results of an absolute measure of agreement of each characteristic included in the CRF for multiple raters [37–39]. Notably, the radiologists were experienced in this specific field of MRI of pediatric renal tumors, and partly selected on their previous scientific contributions. We also acknowledge the fact, that interpreting radiology data remains subjective, it being considerably dependent on the perception of the observer, leaving agreement between raters a critical issue in imaging [70,71]. Despite relatively similar scan protocols on 1.5 T MRIs in our study, scan parameters differ not only on national level, but also on a patient level [70]. Although this will have a small effect on the results in this study, it limits the possibilities for statistical analysis of for instance ADC-values, given the wide range of scanned and used b-values [72]. Altogether this stresses the importance of international collaboration and studies, that may inform universal scan protocols for imaging of pediatric renal tumors [27,73]. Finally, the retrospective cohort design without patients with a WT did not allow for conclusions concerning the discriminative value of MRI in the differentiation of pediatric renal tumor types.

Given the growing preference for MRI for diagnosis and treatment response assessment in pediatric renal tumors over the past years, non-invasive discrimination based on this imaging modality needs to be further explored. This study describes the MRI-characteristics of CCSK and RTK at initial presentation in the largest retrospective series so far through an international SIOP-RTSG collaboration. Differentiation of these rare pediatric renal tumor types from especially the more common WT remains difficult. Nevertheless, RTKs showed a significantly smaller size, more T2W hypo-intensity and an aggressive growth pattern, as compared to CCSKs and potentially WTs. CCSKs showed less potential pathognomonic characteristics, as they seem to resemble MRI-characteristics of stromal WT. However, they do often show a characteristic band-like enhancement pattern. Historically typical metastatic patterns for both CCSK and RTK, although quite discriminative, might not be satisfactory to be of great diagnostic value, since the lungs still seem to be the most common metastatic site for both tumors. Early non-invasive diagnosis based on imaging could be beneficial for increasing outcome of rare non-WT cases as well as WT cases. Future studies may focus on validation and the discriminative value of identified MRI-characteristics for CCSK and RTK, especially aiming for the differentiation from WTs and other rare non-WTs (Table 3).

Table 3
Overview of identified potentially specific magnetic resonance imaging (MRI)- and diffusion weighted imaging (DWI)-characteristics of clear cell sarcoma of the kidney (CCSK) and rhabdoid tumor of the kidney (RTK) in the light of their differentiation from each other and from Wilms tumors (WTs).

Tumor type	Identified potentially specific MRI- and DWI-characteristics of CCSK and RTK	Most common MRI- and DWI-characteristics of WT[a]
CCSK	• Characteristic band-like enhancement pattern • General characteristics resembling stromal type tumor • ADC-values corresponding to a stromal tumor type • Limited venous invasion • Bone metastases besides pulmonary metastases	• (Pseudo)capsule • Large, solid tumor • T1W hypo-intensity • T2W hyper-intensity • Heterogeneous enhancement due to hemorrhagic/necrotic components • Varying ADC-values related to histopathology
RTK	• Younger age[b] • Small size • T2W hypo-intensity • Aggressive growth pattern • High cellularity; low ADC-values • Limited venous invasion • Synchronous tumor / metastases in the brain besides pulmonary metastases	• Possible tumor thrombus • Pulmonary metastases • Bilateral disease

CCSK = clear cell sarcoma of the kidney; RTK = rhabdoid tumor of the kidney; WT = Wilms tumor; MRI = magnetic resonance imaging; DWI = diffusion weighted imaging.
[a] The MRI-characteristics reported in this table are the most common and general characteristics of WT, but the great variety of potentially identifiable characteristics of WTs always needs to be taken into consideration; a non-specific presentation of a WT remains more common than a specific presentation of a non-WT;
[b] Age is not an MRI-characteristic, nevertheless, it might be a discriminating factor to take into consideration combined with the other identified potentially specific MRI- and DWI-characteristics of RTK.

Funding

This work was supported by a grant (grant number 341) from the Stichting Kinderen Kankervrij (KiKa).

Ethical consideration

Informed consent from registration in the International Society of Pediatric Oncology – Renal Tumor Study Group (SIOP-RTSG) SIOP 93–01, SIOP 2001 (SIOP WT 2001 trial, EudraCT number: 2007–004591–39), UK-IMPORT (London Bridge number: 12/LO/0101) and 2016-UMBRELLA (EudraCT number: 2016–004180–39) studies had been obtained from parents of included pediatric patients prior to treatment, according to national law and regulations. In The Netherlands, formal consent for diagnostic MR-images was waived following obtained approval from the Institutional Review Board of the University Medical Center Utrecht (WAG/mb/20/019804 20–332, 26–05–2020) due to the retrospective nature of the study. In Germany, the study was approved of by the Institutional Ethics Committee of the Ärztekammer des Saarlandes (number: 136/01, 20th of September 2002) for SIOP 2001 and concomitant research. This study was approved by the SIOP-RTSG steering committee in 2022.

Declaration of Competing Interest

The authors declare that they have no known competing financial interests or personal relationships that could have appeared to influence the work reported in this paper.

Data availability

The data supporting the findings of this study are available from the International Society of Pediatric Oncology – Renal Tumor Study Group (SIOP-RTSG) office following standard access procedures upon reasonable request.

Appendix A. Supporting information

Supplementary data associated with this article can be found in the online version at doi:10.1016/j.ejcped.2023.100122.

References

[1] M.M. van den Heuvel-Eibrink, J.A. Hol, K. Pritchard-Jones, H. van Tinteren, R. Furtwängler, A.C. Verschuur, G.M. Vujanic, I. Leuschner, J. Brok, C. Rübe, A. M. Smets, G.O. Janssens, J. Godzinski, G.L. Ramírez-Villar, B. de Camargo, H. Segers, P. Collini, M. Gessler, C. Bergeron, F. Spreafico, N. Graf, Position paper: rationale for the treatment of Wilms tumour in the UMBRELLA SIOP-RTSG 2016 protocol, Nat. Rev. Urol. 14 (12) (2017) 743–752, https://doi.org/10.1038/nrurol.2017.163.
[2] G. Pastore, A. Znaor, F. Spreafico, N. Graf, K. Pritchard-Jones, E. Steliarova-Foucher, Malignant renal tumours incidence and survival in European children (1978-1997): report from the Automated Childhood Cancer Information System project, Eur. J. Cancer 42 (13) (2006) 2103–2114, https://doi.org/10.1016/j.ejca.2006.05.010.
[3] P. Roy, S.E. van Peer, M.M. de Witte, G.A.M. Tytgat, H.E. Karim-Kos, M. van Grotel, C.P. van de Ven, A.M.C. Mavinkurve-Groothuis, J.H.M. Merks, R.P. Kuiper, J. A. Hol, G.O.R. Janssens, R.R. de Krijger, M.C.J. Jongmans, J. Drost, A.F.W. van der Steeg, A.S. Littooij, M. Wijnen, H. van Tinteren, M.M. van den Heuvel-Eibrink, Characteristics and outcome of children with renal tumors in the Netherlands: the

first five-year's experience of national centralization, PLoS One 17 (1) (2022), e0261729, https://doi.org/10.1371/journal.pone.0261729.
[4] K. Nakata, M. Colombet, C.A. Stiller, K. Pritchard-Jones, E. Steliarova-Foucher, Incidence of childhood renal tumours: An international population-based study, Int. J. Cancer 147 (12) (2020) 3313–3327, https://doi.org/10.1002/ijc.33147.
[5] A.P. Aldera, K. Pillay, Clear cell sarcoma of the kidney, Arch. Pathol. Lab. Med. 144 (1) (2020) 119–123, https://doi.org/10.5858/arpa.2018-0353-RS.
[6] S.L. Gooskens, R. Furtwängler, G.M. Vujanic, J.S. Dome, N. Graf, M.M. van den Heuvel-Eibrink, Clear cell sarcoma of the kidney: a review, Eur. J. Cancer 48 (14) (2012) 2219–2226, https://doi.org/10.1016/j.ejca.2012.04.009.
[7] K.W. Eaton, L.S. Tooke, L.M. Wainwright, A.R. Judkins, J.A. Biegel, Spectrum of SMARCB1/INI1 mutations in familial and sporadic rhabdoid tumors, Pediatr. Blood Cancer 56 (1) (2011) 7–15, https://doi.org/10.1002/pbc.22831.
[8] M.H. Abu Arja, P. Patel, S.H. Shah, J.J. Auletta, E.K. Meyer, S.E. Conley, J. H. Aldrink, J.A. Pindrik, M.S. AbdelBaki, Synchronous central nervous system atypical teratoid/rhabdoid tumor and malignant rhabdoid tumor of the kidney: case report of a long-term survivor and review of the literature, World Neurosurg. 111 (2018) 6–15, https://doi.org/10.1016/j.wneu.2017.11.158.
[9] S. Alavi, A. Rashidi, A.R. Khatami, M.T. Arzanian, Rhabdoid tumor of the kidney presenting with hemiplegia: report of a case, Pediatr. Hematol. Oncol. 24 (2) (2007) 123–128, https://doi.org/10.1080/08880010601069963.
[10] G.E. Tomlinson, N.E. Breslow, J. Dome, K.A. Guthrie, P. Norkool, S. Li, P. R. Thomas, E. Perlman, J.B. Beckwith, G.J. D'Angio, D.M. Green, Rhabdoid tumor of the kidney in the National Wilms' Tumor Study: age at diagnosis as a prognostic factor, J. Clin. Oncol. 23 (30) (2005) 7641–7645, https://doi.org/10.1200/jco.2004.00.8110.
[11] M.M. van den Heuvel-Eibrink, H. van Tinteren, H. Rehorst, A. Coulombe, C. Patte, B. de Camargo, J. de Kraker, I. Leuschner, R. Lugtenberg, K. Pritchard-Jones, B. Sandstedt, F. Spreafico, N. Graf, G.M. Vujanic, Malignant rhabdoid tumours of the kidney (MRTKs), registered on recent SIOP protocols from 1993 to 2005: a report of the SIOP renal tumour study group, Pediatr. Blood Cancer 56 (5) (2011) 733–737, https://doi.org/10.1002/pbc.22922.
[12] P. Argani, E.J. Perlman, N.E. Breslow, N.G. Browning, D.M. Green, G.J. D'Angio, J. B. Beckwith, Clear cell sarcoma of the kidney: a review of 351 cases from the National Wilms Tumor Study Group Pathology Center, Am. J. Surg. Pathol. 24 (1) (2000) 4–18, https://doi.org/10.1097/00000478-200001000-00002.
[13] W. Friesenbichler, R. Lüftinger, G. Kropshofer, M. Henkel, G. Amann, R. Furtwängler, N. Graf, L. Kager, Clear cell sarcoma of the kidney in Austrian children: long-term survival after relapse, Pediatr. Blood Cancer 68 (5) (2021), e28860, https://doi.org/10.1002/pbc.28860.
[14] S.L. Gooskens, N. Graf, R. Furtwängler, F. Spreafico, C. Bergeron, G.L. Ramírez-Villar, J. Godzinski, C. Rübe, G.O. Janssens, G.M. Vujanic, I. Leuschner, A. Coulomb-L'Hermine, A.M. Smets, B. de Camargo, S. Stoneham, H. van Tinteren, K. Pritchard-Jones, M.M. van den Heuvel-Eibrink, Position paper: rationale for the treatment of children with CCSK in the UMBRELLA SIOP-RTSG 2016 protocol, Nat. Rev. Urol. 15 (5) (2018) 309–319, https://doi.org/10.1038/nrurol.2018.14.
[15] T.J. Jackson, H.J. Brisse, K. Pritchard-Jones, K. Nakata, C. Morosi, T. Oue, S. Irtan, G. Vujanic, M.M. van den Heuvel-Eibrink, N. Graf, T. Chowdhury, How we approach paediatric renal tumour core needle biopsy in the setting of preoperative chemotherapy: a review from the SIOP Renal Tumour Study Group, Pediatr. Blood Cancer (2022), e29702, https://doi.org/10.1002/pbc.29702.
[16] T. Watson, M. Oostveen, H. Rogers, K. Pritchard-Jones, Ø. Olsen, The role of imaging in the initial investigation of paediatric renal tumours, Lancet Child Adolesc. Health 4 (3) (2020) 232–241, https://doi.org/10.1016/s2352-4642(19)30340-2.
[17] Y. de la Monneraye, J. Michon, H. Pacquement, I. Aerts, D. Orbach, F. Doz, F. Bourdeaut, S. Sarnacki, P. Philippe-Chomette, G. Audry, A. Coulomb, P. Fréneaux, J. Klijanienko, D. Berrebi, J.M. Zucker, G. Schleiermacher, H.J. Brisse, Indications and results of diagnostic biopsy in pediatric renal tumors: a retrospective analysis of 317 patients with critical review of SIOP guidelines, Pediatr. Blood Cancer 66 (6) (2019), e27641, https://doi.org/10.1002/pbc.27641.
[18] H. Ueno-Yokohata, H. Okita, K. Nakasato, T. Hishiki, R. Shirai, S. Tsujimoto, T. Osumi, S. Yoshimura, Y. Yamada, Y. Shioda, C. Kiyotani, K. Terashima, O. Miyazaki, K. Matsumoto, N. Kiyokawa, T. Yoshioka, M. Kato, Preoperative diagnosis of clear cell sarcoma of the kidney by detection of BCOR internal tandem duplication in circulating tumor DNA, Genes Chromosomes Cancer 57 (10) (2018) 525–529, https://doi.org/10.1002/gcc.22648.
[19] A.L. Stanescu, P.T. Acharya, E.Y. Lee, G.S. Phillips, Pediatric renal neoplasms:: MR imaging-based practical diagnostic approach, Magn. Reson Imaging Clin. N. Am. 27 (2) (2019) 279–290, https://doi.org/10.1016/j.mric.2019.01.006.
[20] J.N. van der Beek, T.A. Watson, R.A.J. Nievelstein, H.J. Brisse, C. Morosi, H. M. Lederman, A. Coma, M.M. Gavra, K. Vult von Steyern, K. Lakatos, L. Breysem, E. Varga, H. Ducou Le Pointe, M.H. Lequin, J.F. Schäfer, H.J. Mentzel, A.M. Hötker, G. Calareso, S. Swinson, M. Kyncl, C. Granata, M. Aertsen, P.L. Di Paolo, R.R. de Krijger, N. Graf, Ø.E. Olsen, J.P. Schenk, M.M. van den Heuvel-Eibrink, A. S. Littooij, MRI characteristics of pediatric renal tumors: a SIOP-RTSG radiology panel Delphi study, J. Magn. Reson. Imaging (2021), https://doi.org/10.1002/jmri.27878.
[21] K.L. Birkemeier, Imaging of solid congenital abdominal masses: a review of the literature and practical approach to image interpretation, Pediatr. Radiol. 50 (13) (2020) 1907–1920, https://doi.org/10.1007/s00247-020-04678-1.
[22] N.L. Seibel, Y.Y. Chi, E.J. Perlman, J. Tian, J. Sun, J.R. Anderson, M.L. Ritchey, P. R. Thomas, J. Miser, J.A. Kalapurakal, P.E. Grundy, D.M. Green, Impact of cyclophosphamide and etoposide on outcome of clear cell sarcoma of the kidney treated on the National Wilms Tumor Study-5 (NWTS-5), Pediatr. Blood Cancer 66 (1) (2019), e27450, https://doi.org/10.1002/pbc.27450.
[23] J. Li, W. Zhang, H. Hu, Y. Zhang, Y. Wang, H. Gu, D. Huang, Case analysis of 14 children with malignant rhabdoid tumor of the kidney, Cancer Manag. Res. 13 (2021) 4865–4872, https://doi.org/10.2147/cmar.S309274.
[24] F. Tahir, Z. Majid, L.T. Qadar, A. Abbas, M. Raza, Co-existent rhabdoid tumor of the kidney and brain in a male infant: a rare case, Cureus 11 (8) (2019), e5423, https://doi.org/10.7759/cureus.5423.
[25] A. Franco, T.V. Dao, K.N. Lewis, P.W. Biddinger, A case of clear cell sarcoma of the kidney, J. Radiol. Case Rep. 5 (2) (2011) 8–12, https://doi.org/10.3941/jrcr.v5i2.630.
[26] R. Furtwängler, S.L. Gooskens, H. van Tinteren, J. de Kraker, G. Schleiermacher, C. Bergeron, B. de Camargo, T. Acha, J. Godzinski, B. Sandstedt, I. Leuschner, G. M. Vujanic, R. Pieters, N. Graf, M.M. van den Heuvel-Eibrink, Clear cell sarcomas of the kidney registered on International Society of Pediatric Oncology (SIOP) 93-01 and SIOP 2001 protocols: a report of the SIOP Renal Tumour Study Group, Eur. J. Cancer 49 (16) (2013) 3497–3506, https://doi.org/10.1016/j.ejca.2013.06.036.
[27] J.N. van der Beek, M. Artunduaga, J.P. Schenk, M.J. Eklund, E.A. Smith, H. M. Lederman, A.B. Warwick, A.S. Littooij, G. Khanna, Similarities and controversies in imaging of pediatric renal tumors: a SIOP-RTSG and COG collaboration, Pediatr. Blood Cancer (2022), e30080, https://doi.org/10.1002/pbc.30080.
[28] A.S. Littooij, P.G. Nikkels, C.A. Hulsbergen-van de Kaa, C.P. van de Ven, M.M. van den Heuvel-Eibrink, Ø.E. Olsen, Apparent diffusion coefficient as it relates to histopathology findings in post-chemotherapy nephroblastoma: a feasibility study, Pediatr. Radiol. 47 (12) (2017) 1608–1614, https://doi.org/10.1007/s00247-017-3931-9.
[29] P.W. Hales, Ø.E. Olsen, N.J. Sebire, K. Pritchard-Jones, C.A. Clark, A multi-Gaussian model for apparent diffusion coefficient histogram analysis of Wilms' tumour subtype and response to chemotherapy, NMR Biomed. 28 (8) (2015) 948–957, https://doi.org/10.1002/nbm.3337.
[30] B. Laguna, A.C. Westphalen, C.T. Guimarães, Z. Whang, J. Simko, R. Zagoria, Uncommon malignant renal tumors and atypical presentation of common ones: a guide for radiologists, Abdom. Radiol. 44 (4) (2019) 1430–1452, https://doi.org/10.1007/s00261-018-1789-4.
[31] W. Zekri, D. Yehia, M.M. Elshafie, M.S. Zaghloul, N. El-Kinaai, H. Taha, A. Refaat, A.A. Younes, A.S. Alfaar, Bilateral clear cell sarcoma of the kidney, J. Egypt. Natl. Cancer Inst. 27 (2) (2015) 97–100, https://doi.org/10.1016/j.jnci.2015.03.002.
[32] S.G. Farmakis, M.J. Siegel, Rhabdoid tumor: an aggressive renal medullary tumor of childhood, J. Comput. Assist. Tomogr. 39 (1) (2015) 44–46, https://doi.org/10.1097/rct.0000000000000195.
[33] H. Moch, A.L. Cubilla, P.A. Humphrey, V.E. Reuter, T.M. Ulbright, The 2016 WHO classification of tumours of the urinary system and male genital organs-part a: renal, penile, and testicular tumours, Eur. Urol. 70 (1) (2016) 93–105, https://doi.org/10.1016/j.eururo.2016.02.029.
[34] A. Lopez-Beltran, M. Scarpelli, R. Montironi, Z. Kirkali, 2004 WHO classification of the renal tumors of the adults, Eur. Urol. 49 (5) (2006) 798–805, https://doi.org/10.1016/j.eururo.2005.11.035.
[35] J.N. Eble, G. Sauter, J.I. Epstein, I.A. Sesterhenn, World Health Organization Classification of Tumours. Pathology and Genetics of Tumours of the Urinary System and Male Genital Organs IARC Press, IARC Press, 2004.
[36] E. Bruder, O. Passera, D. Harms, I. Leuschner, M. Ladanyi, P. Argani, J.N. Eble, K. Struckmann, P. Schraml, H. Moch, Morphologic and molecular characterization of renal cell carcinoma in children and young adults, Am. J. Surg. Pathol. 28 (9) (2004) 1117–1132.
[37] H.C.W. de Vet, R.E. Dikmans, I. Eekhout, Specific agreement on dichotomous outcomes can be calculated for more than two raters, J. Clin. Epidemiol. 83 (2017) 85–89, https://doi.org/10.1016/j.jclinepi.2016.12.007.
[38] H.C. de Vet, L.B. Mokkink, C.B. Terwee, O.S. Hoekstra, D.L. Knol, Clinicians are right not to like Cohen's κ, BMJ 346 (2013) f2125, https://doi.org/10.1136/bmj.f2125.
[39] H.C.W. de Vet, M.G. Mullender, I. Eekhout, Specific agreement on ordinal and multiple nominal outcomes can be calculated for more than two raters, J. Clin. Epidemiol. 96 (2018) 47–53, https://doi.org/10.1016/j.jclinepi.2017.11.024.
[40] J. Kottner, L. Audigé, S. Brorson, A. Donner, B.J. Gajewski, A. Hróbjartsson, C. Roberts, M. Shoukri, D.L. Streiner, Guidelines for Reporting Reliability and Agreement Studies (GRRAS) were proposed, J. Clin. Epidemiol. 64 (1) (2011) 96–106, https://doi.org/10.1016/j.jclinepi.2010.03.002.
[41] M. Benchoufi, E. Matzner-Lober, N. Molinari, A.S. Jannot, P. Soyer, Interobserver agreement issues in radiology, Diagn. Interv. Imaging 101 (10) (2020) 639–641, https://doi.org/10.1016/j.diii.2020.09.001.
[42] N. Gisev, J.S. Bell, T.F. Chen, Interrater agreement and interrater reliability: key concepts, approaches, and applications, Res. Soc. Adm. Pharm. 9 (3) (2013) 330–338, https://doi.org/10.1016/j.sapharm.2012.04.004.
[43] J.R. Landis, G.G. Koch, An application of hierarchical kappa-type statistics in the assessment of majority agreement among multiple observers, Biometrics 33 (2) (1977) 363–374.
[44] M. Hirose, K. Mizuno, H. Kamisawa, H. Nishio, Y. Moritoki, K. Kohri, Y. Hayashi, Clear cell sarcoma of the kidney distinguished from synovial sarcoma using genetic analysis: a case report, BMC Res. Notes 8 (2015) 129, https://doi.org/10.1186/s13104-015-1100-5.
[45] H.E. Trejo Bittar, J.E. Radder, S. Ranganathan, A. Srinivasan, S. Madan-Khetarpal, M. Reyes-Mugica, Clear cell sarcoma of the kidney in a child with Fanconi anemia, Pediatr. Dev. Pathol. 17 (4) (2014) 297–301, https://doi.org/10.2350/14-03-1450-cr.1.
[46] R. Sharma, B.J. Kitchen, R. Mody, A. Chamdin, S. Bruch, R. Jasty, A report of renal artery embolization for hematuria facilitating neoadjuvant chemotherapy in an

unresectable malignant renal rhabdoid tumor, Pediatr. Surg. Int. 29 (5) (2013) 533–535, https://doi.org/10.1007/s00383-013-3260-5.
[47] F. Eftekhari, W.K. Erly, N. Jaffe, Malignant rhabdoid tumor of the kidney: imaging features in two cases, Pediatr. Radiol. 21 (1) (1990) 39–42, https://doi.org/10.1007/bf02010812.
[48] C.J. Chung, D. Cammoun, M. Munden, Rhabdoid tumor of the kidney presenting as an abdominal mass in a newborn, Pediatr. Radiol. 20 (7) (1990) 562–563, https://doi.org/10.1007/bf02011394.
[49] E.M. Chung, G.E. Lattin Jr., K.E. Fagen, A.M. Kim, M.A. Pavio, A.J. Fehringer, R. M. Conran, Renal tumors of childhood: radiologic-pathologic correlation part 2. The 2nd decade: from the radiologic pathology archives, Radiographics 37 (5) (2017) 1538–1558, https://doi.org/10.1148/rg.2017160189.
[50] L.H. Lowe, B.H. Isuani, R.M. Heller, S.M. Stein, J.E. Johnson, O.M. Navarro, M. Hernanz-Schulman, Pediatric renal masses: Wilms tumor and beyond, Radiographics 20 (6) (2000) 1585–1603, https://doi.org/10.1148/radiographics.20.6.g00nv051585.
[51] J.B. Beckwith, N.F. Palmer, Histopathology and prognosis of Wilms tumors: results from the First National Wilms' Tumor Study, Cancer 41 (5) (1978) 1937–1948, https://doi.org/10.1002/1097-0142(197805)41:5<1937::aid-cncr2820410538>3.0.co;2-u.
[52] E. Morgan, J.M. Kidd, Undifferentiated sarcoma of the kidney: a tumor of childhood with histopathologic and clinical characteristics distinct from Wilms' tumor, Cancer 42 (4) (1978) 1916–1921, https://doi.org/10.1002/1097-0142(197810)42:4<1916::aid-cncr2820420433>3.0.co;2-r.
[53] H.B. Marsden, W. Lawler, P.M. Kumar, Bone metastasizing renal tumor of childhood: morphological and clinical features, and differences from Wilms' tumor, Cancer 42 (4) (1978) 1922–1928, https://doi.org/10.1002/1097-0142(197810)42:4<1922::aid-cncr2820420434>3.0.co;2-z.
[54] H. Fukushima, K. Yamasaki, M. Sakaida, N. Tsujio, T. Okuno, N. Ishii, K. Okada, H. Fujisaki, Y. Matsusaka, H. Sakamoto, A. Yoneda, J. Hara, T. Inoue, Rhabdoid tumor predisposition syndrome with renal tumor 10 years after brain tumor, Pathol. Int. 71 (2) (2021) 155–160, https://doi.org/10.1111/pin.13056.
[55] S. Park, J.H. Seo, J.B. Park, S. Park, Malignant rhabdoid tumor of the kidney and spine in an infant, J. Korean Neurosurg. Soc. 55 (1) (2014) 57–60, https://doi.org/10.3340/jkns.2014.55.1.57.
[56] S. Swinson, K. McHugh, Urogenital tumours in childhood, Cancer Imaging 11 Spec No A (1a) (2011) S48–64, https://doi.org/10.1102/1470-7330.2011.9009.
[57] M. Powis, Neonatal renal tumours, Early Hum. Dev. 86 (10) (2010) 607–612, https://doi.org/10.1016/j.earlhumdev.2010.08.018.
[58] G. Khanna, A. Naranjo, F. Hoffer, E. Mullen, J. Geller, E.J. Gratias, P.F. Ehrlich, E. J. Perlman, N. Rosen, P. Grundy, J.S. Dome, Detection of preoperative wilms tumor rupture with CT: a report from the Children's Oncology Group, Radiology 266 (2) (2013) 610–617, https://doi.org/10.1148/radiol.12120670.
[59] C.J. Chung, R. Lorenzo, S. Rayder, E. Schemankewitz, C.D. Guy, J. Cutting, M. Munden, Rhabdoid tumors of the kidney in children: CT findings, AJR Am. J. Roentgenol. 164 (3) (1995) 697–700, https://doi.org/10.2214/ajr.164.3.7863897.
[60] T.I. Han, M.J. Kim, H.K. Yoon, J.Y. Chung, K. Choeh, Rhabdoid tumour of the kidney: imaging findings, Pediatr. Radiol. 31 (4) (2001) 233–237, https://doi.org/10.1007/s002470000417.
[61] G.A. Agrons, K.D. Kingsman, B.J. Wagner, C. Sotelo-Avila, Rhabdoid tumor of the kidney in children: a comparative study of 21 cases, AJR Am. J. Roentgenol. 168 (2) (1997) 447–451, https://doi.org/10.2214/ajr.168.2.9016225.
[62] M. Aslan, A. Aslan, H. Arıöz Habibi, A. Kalyoncu Uçar, E. Özmen, S. Bakan, S. Kuruğoğlu, İ. Adaletli, Diffusion-weighted MRI for differentiating Wilms tumor from neuroblastoma, Diagn. Interv. Radiol. 23 (5) (2017) 403–406, https://doi.org/10.5152/dir.2017.16541.
[63] J.P. Schenk, N. Graf, P. Günther, S. Ley, M. Göppl, A. Kulozik, W.K. Rohrschneider, J. Tröger, Role of MRI in the management of patients with nephroblastoma, Eur. Radiol. 18 (4) (2008) 683–691, https://doi.org/10.1007/s00330-007-0826-4.
[64] A. Ooms, G.M. Vujanić, E. D'Hooghe, P. Collini, A. L'Herminé-Coulomb, C. Vokuhl, N. Graf, M. Heuvel-Eibrink, R.R. de Krijger, Renal tumors of childhood-a histopathologic pattern-based diagnostic approach, Cancers 12 (3) (2020), https://doi.org/10.3390/cancers12030729.
[65] M.S. Gee, M. Bittman, M. Epelman, S.O. Vargas, E.Y. Lee, Magnetic resonance imaging of the pediatric kidney: benign and malignant masses, Magn. Reson Imaging Clin. N. Am. 21 (4) (2013) 697–715, https://doi.org/10.1016/j.mric.2013.06.001.
[66] E.M. Chung, A.R. Graeber, R.M. Conran, Renal tumors of childhood: radiologic-pathologic correlation part 1. The 1st decade: from the radiologic pathology archives, Radiographics 36 (2) (2016) 499–522, https://doi.org/10.1148/rg.2016150230.
[67] A.S. Littooij, N.J. Sebire, Ø.E. Olsen, Whole-tumor apparent diffusion coefficient measurements in nephroblastoma: can it identify blastemal predominance? J. Magn. Reson Imaging 45 (5) (2017) 1316–1324, https://doi.org/10.1002/jmri.25506.
[68] A.M. Hötker, A. Lollert, Y. Mazaheri, S. Müller, J.P. Schenk, P.C. Mildenberger, O. Akin, N. Graf, G. Staatz, Diffusion-weighted MRI in the assessment of nephroblastoma: results of a multi-center trial, Abdom. Radiol. 45 (10) (2020) 3202–3212, https://doi.org/10.1007/s00261-020-02475-w.
[69] P.D. Humphries, N.J. Sebire, M.J. Siegel, Ø.E. Olsen, Tumors in pediatric patients at diffusion-weighted MR imaging: apparent diffusion coefficient and tumor cellularity, Radiology 245 (3) (2007) 848–854, https://doi.org/10.1148/radiol.2452061535.
[70] G. Di Leo, Measurements in radiology: the need for high reproducibility, Pediatr. Radiol. 45 (1) (2015) 32–34, https://doi.org/10.1007/s00247-014-3081-2.
[71] A.A. Bankier, D. Levine, E.F. Halpern, H.Y. Kressel, Consensus interpretation in imaging research: is there a better way? Radiology 257 (1) (2010) 14–17, https://doi.org/10.1148/radiol.10100252.
[72] C. Chatziantoniou, R.A. Schoot, R. van Ewijk, R.R. van Rijn, S.A.J. Ter Horst, J.H. M. Merks, A. Leemans, A. De Luca, Methodological considerations on segmenting rhabdomyosarcoma with diffusion-weighted imaging-What can we do better? Insights Imaging 14 (1) (2023) 19, https://doi.org/10.1186/s13244-022-01351-z.
[73] M.M. van den Heuvel-Eibrink, C.V. Fernandez, N. Graf, J.I. Geller, Progress by international collaboration for pediatric renal tumors by HARMONIzation and COllaboration: the HARMONICA initiative, Pediatr. Blood Cancer 70 (Suppl 2) (2023), e30082, https://doi.org/10.1002/pbc.30082.